NJOC-CP(16) 15392

A Shepherd et al.

Modelling and Analysis of the JET EP2 Neutral Beam Full Energy Ion Dump Curved End Plate

Preprint of Paper to be submitted for publication in
Proceedings of 29th Symposium on Fusion Technology (SOFT 2016)

This work has been carried out within the framework of the Contract for the Operation of the JET Facilities and has received funding from the European Unions Horizon 2020 research and innovation programme. The views and opinions expressed herein do not necessarily reflect those of the European Commission.

Modelling and Analysis of the JET EP2 Neutral Beam Full Energy Ion Dump Curved End Plate

Alastair John Shepherd[a], I.E. Day[a], P. Blatchford[a], S. Cooper[a], R. Marshall[a], G. Pérez[a], E. Swatton[a], S. Robinson[a], I.Turner[a], Y. Xue[a], J.Zacks[a], A. Tallarigo[a] and R.McAdams[a]

[a]*CCFE, Culham Science Centre, Abingdon, Oxon, OX14 3DB, UK*

This paper describes enhanced modelling of the power loading on the current JET full energy ion dump (FEID) curved end plate, and the new end plate design with improvements to the power handling capabilities and additional features to improve fatigue life. Monte-Carlo simulations of each of the nine residual ion components which are intercepted by the plate shows a peak power density of 25MW/m^2 and compares well with recently installed fast thermocouple measurements. Analytical calculations and simulations with the Charged Particle Optics (CPO) code are used to investigate the potential for movement of the residual ion focus due to space charge effects. Cooling performance is significantly enhanced by improved water channel flow which is both modelled and confirmed by experiment. Fatigue life, calculated from ANSYS modelling is improved using a slot arrangement to relieve stresses created from focussed heat load distribution.

Keywords: JET, NBI, curved end plate, ion dump, thermal analysis, structural analysis

1. Introduction

Neutral beam injection systems have proved themselves as the most effective form of auxiliary heating in tokamak plasmas. In positive ion based systems once the beam is neutralised there are many residual ion components which must be intercepted by suitable ion dumps. A particular challenge for ion dump design occurs when the dump must be placed close to a focus point as is the case for the curved end plate of the JET NBI full energy ion dump. Molecular ion species, though of low power, are focused 30cm in front of this plate.

As part of the EP2 upgrade to increase neutral beam power and duration, the ion source configuration was changed from Supercusp 130kV/60A configuration to Chequerboard 125kV/65A [1]. This allowed for significant increase in neutral beam power but also lead to a fourfold increase in molecular residual ions. The curved FEID end plate was re-designed as an actively cooled element using swirl tubes. Following a failure of this plate in 2014 additional analysis was carried out to determine the power loading on the plate and to improve its performance.

2. Current end plate modelling and analysis

2.1 Monte-Carlo simulations

Modelling of the power loading on the curved FEID end plate carried out in support of the EP2 upgrade predicted a peak power loading of 10MW/m^2. However, this was not done for each individual ion species and did not take into account the depletion of the neutraliser target density at high voltages. This increases the proportion of residual ion species produced in the neutraliser region and thus the power loading on the end plate.

Power loading in the JET beamline is modelled by quadrant using the MAGNET code, a Monte-Carlo simulation program. Each quadrant contains an end plate, which in MAGNET is modelled as five discontinuous plates tangent to the outer face as shown in figure 1, and two Positive Ion Neutral Injectors (PINIs). The power loading incident on the end plate was modelled for each individual residual ion and re-ionised ion species for the two PINIs operating in 125kV/65A Deuterium.

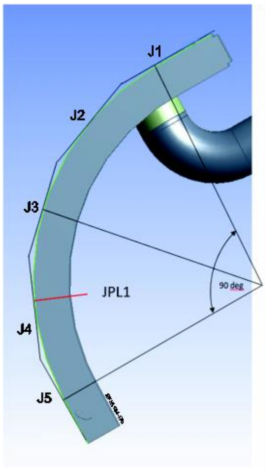

Fig. 1. Curved FEID end plate with the 5 plates used in MAGNET. JPL1 is the newly installed fast thermocouple.

The highest peak power density was found to be 25MW/m^2 on the quadrant 1 (Q1) curved end plate

Author's email: Alastair.Shepherd@ukaea.uk

as seen in figure 2. This is to be expected as PINI 1 in Q1 is upshifted, decreasing the angle between the beam and the central beamline axis and moving the beam closer to the end plate. The largest contribution comes from the PINI 1 D_2+ full energy ions, followed by D_3+ full energy ions. PINI 2, being the upper PINI in the quadrant has no residual ion contribution as the full energy ions are bent onto the far side of the FEID. Both PINIs contribute several MW/m^2 through re-ionised power loading, however this is less focussed as the ions do not all originate from the neutraliser as the residual ions do.

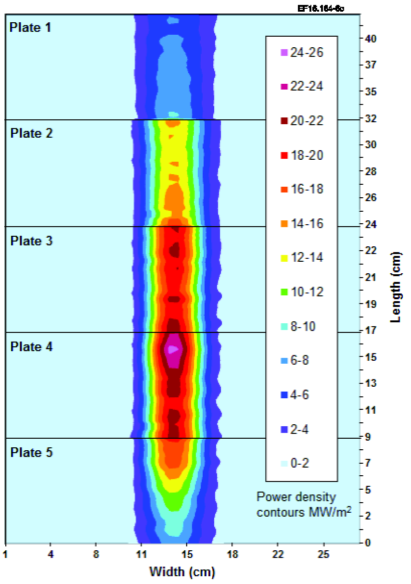

Fig. 3. MAGNET power density profile for the Q1 curved FEID end plate. Peak power density of 25 MW/m^2

2.2 Charged Particle Optics

MAGNET does not take into account space charge, which could potentially move the residual ion focus point closer to the end plate and result in a higher peak power density. The CPO code [2] was used to model this effect. CPO was run for the D_2+ residual ion species, as the largest contributor to the power loading. The degree of space charge was varied from 0-0.15%, with little change to the focus point of the ions. The 25MW/m^2 simulated by MAGNET for Q1 is therefore taken as a worst case for the rest of this paper.

2.3 Fast thermocouple measurements

To monitor the temperature of the existing end plates a new fast thermocouple was positioned close to the surface during the 2015 shutdown as shown in figure 1. This gives a more accurate reading of the surface temperature in the area of high power loading as given by MAGNET.

Initial analysis was performed using a simple 1D heat transfer model [3] for a copper chrome zirconium plate with temperature dependent conductivity. No cooling of the back surface was assumed, thus only the first 500ms of pulses were used, as after that the effect of the plate's active cooling is seen. Firstly the thermocouple depth was fitted and averaged over several pulses. This was then input into the model as a fixed quantity and the power density obtained by measuring dT over the linear section of the temperature rise curve.

Figure 3 shows the power density for Q1, scaled to the MAGNET beam current and extrapolated to 125kV. At lower voltages the fixed averaged depth was used, but at higher voltages the depth varied enough that it was fitted for each pulse. The 1D power density reaches over 30MW/m^2 at 125kV. This is compared to the MAGNET result, which has been scaled with beam voltage. The ratio of the two power densities is constant over the voltage range, suggesting the neutraliser target depletion applied in MAGNET is largely correct. The thermocouple depth was calculated to be ~7mm deep, greater than the designed depth of 3mm. As the drilling has only ±0.5mm tolerance further analysis was carried out using an ANSYS Workbench model [4].

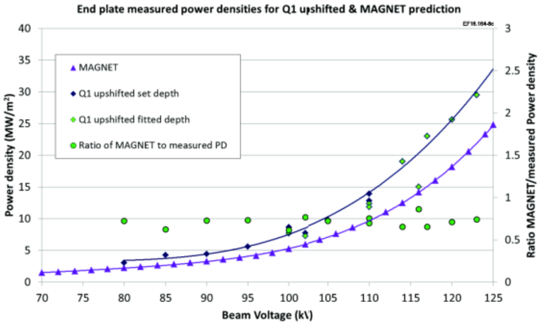

Fig. 3. Normalised Power density plots for the quadrant 1 end plate in upshifted alignment for a range of beam voltages, including MAGNET predictions and ratios of MAGNET to measured power density.

For the ANSYS modelling of the Q1 fast thermocouple two JET pulses were looked at; #89253 and #89257. In each case the MAGNET power density and the water flow, obtained from an ANSYS CFD model, were scaled so that the modelled thermocouple response matched experimental data. This is shown in figure 4. Instead of using a depth of 7mm a better fit was obtained with a nominal depth of 3mm and a thermal conductance of 3000W/m^2 introduced between the thermocouple and the alloy. This is more likely than an incorrect thermocouple depth as a thermal resistance could have been introduced during the welding process. The close match indicates that the ANSYS model gives a good approximation of the Q1 end pate thermal response.

Author's email: Alastair.Shepherd@ukaea.uk

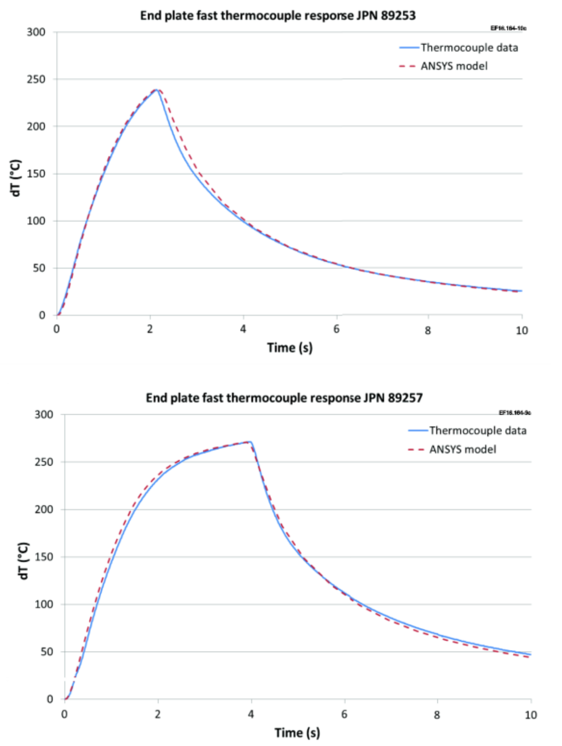

Fig. 4. ANSYS thermocouple profile compared to fast thermocouple data for JET pulse a) #89253, 110kV/40A 2.1s and b) #89257, 110kV/41A 3.9s.

3. New curved end plate design

3.1 Cooling efficiency

Previous analysis of the current curved FEID end plate has determined that the water flow rate through the swirl tubes is too low and unevenly distributed to cope with the expected power loading. For the new plate several structural changes were made to improve cooling efficiency, while maintaining the same cooling system and basic configuration of the current plate. The swirl tubes were redistributed towards the bottom of the plate, where the power density is higher, with the overall number of swirl tubes decreased from 20 to 17. The feed pipes were changed to have a uniform inner diameter of 37.2mm, with fewer bends and the inlet/outlet relocated to the centre of the manifolds. The manifolds themselves were increased in cross sectional area from 27mm x 13mm to 60mm x 18mm. The changes made from the original plate are shown in figure 5.

Using ANSYS CFX 15.0 the water flow through the new design was compared to the current end plate, shown in figure 6. The minimum water flow velocity has increased from 1.22m/s to 3.47 m/s, with the variation in velocity between swirl tubes decreased from 1.85m/s to 0.67m/s. The new design was tested by building a flat acrylic replica of the new end plate, with even water flow through the swirl tubes observed.

Author's email: Alastair.Shepherd@ukaea.uk

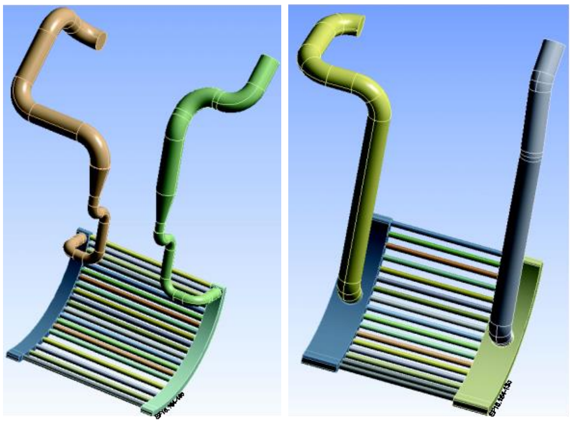

Fig. 5. Cooling structure of a) old FEID curved end plate, b) new FEID curved end plate.

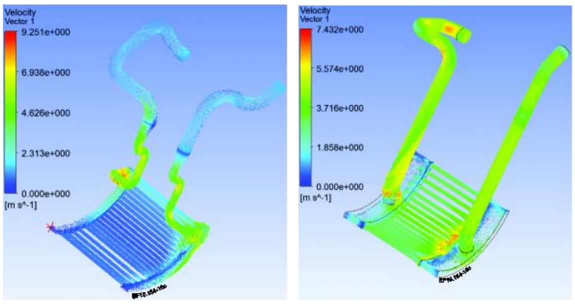

Fig. 6. Water flow velocity vector plots for a) old FEID curved end plate and b) new FEID curved end plate.

3.2 Thermal analysis

Thermal analysis of the new end plate was performed using ANSYS Mechanical 15.0. The MAGNET power density profile was applied to an ANSYS model and then scaled to give a range of power loadings. The swirl tube heat transfer uses correlations developed for ITER divertor and neutral beam swirl tube components [5].

For an applied power density ranging from 10MW/m^2 the transient temperature at time t = 20s was determined, as given in figure 7.

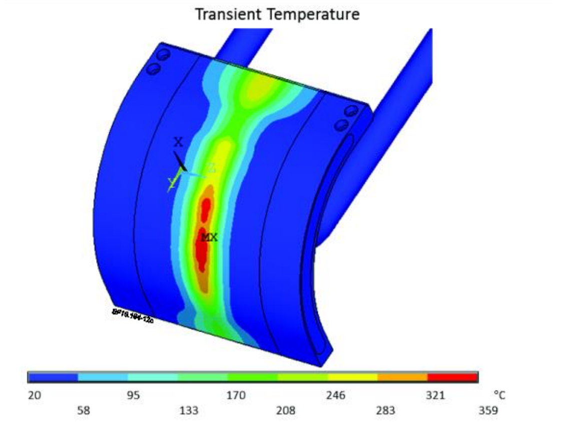

Fig. 7. Transient temperature under 10MW/m^2 power density at time 20s. Peak temperature is 358.5^{o}C.

3.3 Fatigue life

The power loading results in high compressive stress along the middle of the plate's outer surface, and therefore high strain. The result is a fatigue life of only 1300 cycles with an incident power density of 10MW/m^2, well below the required 15,000 cycles. To reduce the strain eight slots were introduced through the plate, one between every two swirl tubes. The slots allow each section to bow out of the plane of the plate, alleviating the strain. The maximum strain is located at the holes located at the end of the slots, as is shown in figure 8.

Table 1 gives the maximum surface temperature, Von Mises stress, strain and fatigue life for a peak power density in the range 10-15MW/m^2. With slotting, the fatigue life for 10MW/m^2 loading increases from 1300 to 25,800 cycles. This falls to 2000 cycles at 15MW/m^2.

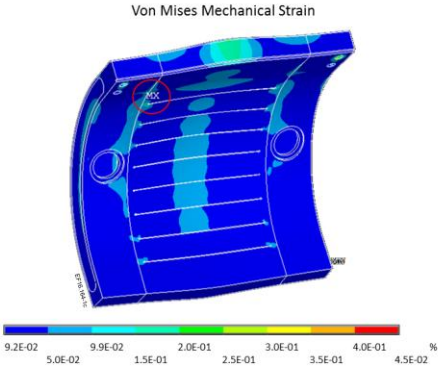

Fig. 8. Von Mises mechanical strain under 15MW/m^2 power density. The maximum strain at the slot hole is circled.

Localised heating of the slot edges was investigated by applying a power density profile normal to the direction of the main power contributions, the D_2+ and D_3+ ions, and any direct interception due to a potentially shallow angle relative to the plate. Scaled to 10MW/m^2 this gives a higher local transient temperature at the slot edge of 407°C. Structural analysis however gives very little change to the fatigue life and therefore heating of the slot edges has little impact on the plate.

Table 1. Temperature, stress, strain and fatigue life for 10-15MW/m ^{2} power density range.

Peak power density (MW/m^2)	**Peak surface temp. (°C)**	**Max Von Mises stress (MPa)**	**Max Von Mises Mechanical strain (%)**	**Fatigue life (cycles)**
10	359	218	0.26	25800
11	381	223	0.28	14900
12	403	227	0.32	9200
13	425	230	0.36	5800
14	446	232	0.40	3400
15	467	235	0.45	2000

Author's email: Alastair.Shepherd@ukaea.uk

4. Conclusion

Following the 2014 failure of the FEID curved end plate Monte-Carlo analysis has determined that up to 25MW/m^2 of power is incident on the plate, mostly from D_2+ and D_3+ full energy ions. Analysis of newly installed fast thermocouple data has confirmed the thermal behaviour of plate.

Based on high power loading and poor water flow in the current plate as the causes of the failure a new FEID curved end plate has been designed. Structural changes have increased the minimum water velocity to 3.47m/s, greatly increasing the cooling efficiency of the plate. By introducing a slotting arrangement the fatigue life of the plate has been determined for a number of applied power densities, giving an initial operational range for the new plates.

The new curved FEID end plates will be installed in the JET NBI system during the 2016-17 shutdown. A new array of surface thermocouples will allow further analysis of the power loading and confirm the thermal behaviour of the plates.

Acknowledgements

This work was part-funded by the RCUK Energy Programme [grant number EP/I501045]. It has been carried out within the framework of the Contract for the Operation of the JET Facilities and has received funding from the European Union's Horizon 2020 research and innovation programme. The views and opinions expressed herein do not necessarily reflect those of the European Commission.

References

[1] D. Ciric et al., Performance of upgraded neutral beam injectors, Fusion Engineering and Design 86 (2011) 509-512.

[2] F. H. Read and N. J. Bowring, The CPO programs and the BEM for charged particle optics, Nuclear Instruments and Methods in Physics Research A645 (2011) 273-277.

[3] I.E. Day and S. Gee, Direct measurement of neutral/ion beam power using thermocouple analysis, Fusion Engineering and Design 82 (2007) 806-812.

[4] A. Tallarigo et al., Thermal analysis exploring damage and operating limits of the J-plate heat exchanger for JET tokamak, to be published in Fusion Engineering and Design.

[5] ITER Design Description Document, DDD 5.3. (N53 DDD 29 01-07-03 R 0.1.), Appendix A.